ELSEVIER

Biophysical Chemistry 61 (1996) 51–58

Biophysical Chemistry

Magnesium-aided folding of group I ribozymes with a minimal loss of entropy

Ariel Fernández, Gustavo Appignanesi

Instituto de Matemática de Bahía Blanca (INMABB), Consejo Nacional de Investigaciones Científicas y Técnicas, Universidad Nacional del Sur, Av. Alem 1253, Bahía Blanca 8000, Argentina

Received 11 March 1996; accepted 13 May 1996

Abstract

The aim of this work is to quantify, rationalize and incorporate the effect of Mg(II) ions on the kinetic barriers of entropic origin associated to RNA folding events in vitro. This study encompasses the scaffolding effect of Mg(II) upon the formation of the pseudoknot structural motif which is believed to be crucial for shaping the catalytic core of group I ribozymes. Our results are contrasted with recent experimental probes on folding kinetics.

The first set of objectives is accomplished by determining the participation of Mg(II) in the reduction of the conformational entropy cost during folding. First, the dominant contribution to conformational entropy loss associated to loop closure is obtained. The derivation hinges upon the notion that loop closure entails the formation of an inner and outer solvent domain and backbone phosphate groups orient themselves concurrently towards the best dielectric environment. At this point, the role of Mg(II) ions can be assessed by taking into account that Mg(II) coordinates with two adjacent backbone phosphates in unpaired regions. Thus, for a small loop of even length, the energy decrease due to coordination reduces the conformational entropy loss due to phosphate orientation by one half.

In the case of pseudoknot formation, the orientational effect prevents the coplanarity of the loops comprising the pseudoknot and allows us to determine the kinetic barrier associated to its formation in the presence of magnesium.

Incorporating these facts to kinetically controlled Monte Carlo simulations, we find that the predicted folding pathway for group I introns leads to the phylogenetically inferred secondary structures and allows us to elucidate the magnesium-dependent rate-limiting step in the formation of the P3-P7 pseudoknotted region of the catalytic core.

Keywords: RNA folding; Ribozyme; Loop closure; Monte Carlo simulation; Pseudoknot

1. Introduction

There is burgeoning interest in the experimental verification of biopolymer folding pathways followed under renaturation conditions in vitro [1–11]. This research is paramount to elucidate the expedient by which natural biopolymers find their active conformation in a robust and expeditive way. From a theoretical perspective, at least three major issues need to be dealt with: 1) The need to minimize the entropic cost, as each folding step entails a loss in conformational entropy [5,6,10]; 2) the severe time constraints under which the search for the active conformation occurs [1–10]; and 3) the fact that the Levinthal-type scenario of exhaustive search in conformation space [4] cannot actually be realized and is

PII S0301-4622(96)02190-4

circumvented by natural biopolymers. These issues led one of the authors to conjecture that the process evolves through an action-directed pathway [5,6]. In this context there is a concrete need to determine the landscape of activation energy barriers [7–9] as the molecule performs a search in conformation space following a least-action principle. This implies that the lowest barriers locally dictate the favored folding step at each stage.

The recognition of the entropic nature of the kinetic barriers associated to intramolecular folding events [5,10], together with a precise determination of the conformational entropy loss associated with loop formation made possible the generation of folding pathways that may be probed experimentally [3,11]. This approach, based on the sequential minimization of the entropy loss (SMEL) has been specialized and applied for RNA folding in vitro [10].

In the present work we specialize the SMEL-based approach to the problem of folding group I ribozymes [12] within an experimentally testable set-up [3]. This context demands that we consider the formation of a tertiary structure motif, the pseudoknot, which plays a pivotal role in catalytic activity [3,12–14] and that we incorporate quantitatively the role of magnesium in lowering the kinetic barriers for folding steps, specifically focusing on the barriers of formation of the pseudoknot. These issues, whose paramount relevance has been revealed by recent experimental kinetic evidence [3] are here for the first time rationalized and incorporated within a theoretical approach.

It has been experimentally found that Mg(II) ions accelerate the folding process and even that the presence of magnesium is essential for group I introns in order to fold properly in the active conformation. In particular, the P3-P7 pseudoknot formation was found to require magnesium in the rate-limiting step in the folding of such introns. These facts are addressed in this work from a theoretical perspective by computing the differential conformational entropy loss entailed by the participation of Mg(II) on elementary folding events.

The plan of the work is as follows: in Section 2 we describe briefly the orientational arguments necessary to derive the conformational entropy loops associated with folding events and we describe the SMEL principle as stated previously [10]. In that section we also extend the theory to incorporate the role of magnesium and the formation of the pseudoknot motif and we describe the implementation of the SMEL-based algorithm through kinetically controlled Monte Carlo simulations. Section 3 is devoted to the discussion of the results obtained for two group I ribozymes. We end that section contrasting our results with recent experimental kinetic findings.

2. Methodology

SMEL control implies that the biopolymer chain folds itself forming at each stage as many intrachain contacts as possible at the expense of a minimal loss in conformational freedom [10]. If we denote the loss in conformational entropy associated with loop closure $\Delta S_{\text{loop},}$ and the number of intrachain effective contacts formed concurrently with such an event n, the SMEL principle requires the minimization of the following quantity at each stage of the folding pathway [10]:

$$Q = n^{-1}\exp(-\Delta S_{\text{loop}}/R) \tag{1}$$

The unimolecular rate constant for the folding step is actually proportional to Q^{-1} [5–11]. This result hinges upon the fact that the kinetic barriers for loop closure are estimated as $-T\Delta S_{\text{loop}}$ [5–10]. The application of the SMEL principle requires a proper derivation of the entropic contribution for any loop size. This has only been achieved for moderately large loops by means of the Jacobson–Stockmayer approximation which yields the well-known result [13]:

$$\Delta S_{\text{loop}} = (-3/2)R\ln N + R\ln\left[(3\pi l^2/2)^{3/2} v\right] \tag{2}$$

where N is the size of the loop, l is the effective length of a monomer and v is the effective contact volume within which two monomers are assumed to have made contact. In a good solvent where excluded-volume effects are to be taken into account, the logarithmic dependence on N must be corrected to $-\mu R \ln N$, with $\mu \approx 1.75$ [13].

This result cannot be extrapolated to small loops where discrete solvent structure effects occur [10,13]. Consider a biopolymer capable of selectively orienting its charged or polar moieties immersed in water.

Upon formation of a loop we are left with two domains of the solvent: an inner confined domain and an outer domain. For small loops, the inner domain acquires discrete features and becomes a poorer dielectric than the bulk-like outer domain. This fact forces the polyelectrolytic chain to orient its charged or polar moieties (phosphates in the case of RNA) towards the outer domain where they can be better solvated.

There is a critical loop size N_0 beyond which both domains behave indistinguishably and each polar or charged group of the chain can adopt both configurations: pointing outwards or inwards. Thus, the orientational entropy contribution drops to zero beyond the critical size. In the case of RNA, the critical value was estimated to be $N_0 \approx 17$ (a loop comprising 17 unpaired nucleotides in between the regions in contact) in the case of a planar loop. This result is obtained considering molecular dimensions and regarding the chain as a rod of fixed cross-section [10].

This separation of domains for small loops must be reflected in the profile $-T\Delta S_{\text{loop}}$ versus N since it represents a restriction in the number of conformations available to the chain. Thus, for RNA we obtain the following reduction in the conformational entropy:

$$\Delta S_{\text{orient}} = R\ln(\Omega'/\Omega)$$
$$= R\ln(2^{M-N}/2^{M}) = -RN\ln 2$$
$$\Delta S_{\text{loop}} \approx -\mu R\ln N - RN\ln 2, \qquad (3)$$

where Ω' is the number of conformations with the ends of the loop constrained to be in contact with one other, Ω is the total number of available conformations, M is the length of the free chain and N is the length of the loop. A plot of the profile of $-T\Delta S_{\text{loop}}$ versus N is shown in Fig. 1.

The incorporation of Eqs. (2) and (3) makes possible the implementation of a SMEL-based algorithm to predict RNA folding pathways. However, in order to place it within the specific experimental context relevant to group I RNA catalysis [12], two features inherent to the folding of group I ribozymes need to be considered: the formation of the pseudoknot motif [3,14] relevant to the shaping of the catalytic core, and 2) the role of magnesium ions on the folding process [3,15].

2.1. Pseudoknot formation

The formation of a pseudoknot occurs when residues in a hairpin loop engage in further base-pairing with residues outside the hairpin forming an additional stem and loop region [14]. As we shall presently see using orientational arguments, the pseudoknot motif cannot lie on a plane, thus it must form a "pocket" or "hinge-like" spatial motif which seems to be essential for catalytic activity. Furthermore, the activation barrier for pseudoknot formation can easily be obtained from the same orientational arguments. Suppose the generic hairpin I has been formed (see Fig. 2) and we need the activation barrier associated with forming loop II, and suppose that loop I and loop II are below the critical range. We first observe that both loops cannot be coplanar since the common region (thick solid line in Fig. 2) has been already oriented upon formation of loop I and, as such, it is solvated by bulk water, a condition not easily relinquished. Should loop II form coplanarly, it would affect the self energy of hydration of the phosphates in the thick line common region by drastically reducing the dielectric in which these phosphates have been previously immersed. Thus, the loops should be formed in the non-coplanar manner suggested by Fig. 2 and $-T\Delta S_{\text{orient}}$ for loop II should be equal to $RTL\ln 2$; where L is the number of nucleotides exclusively belonging to loop

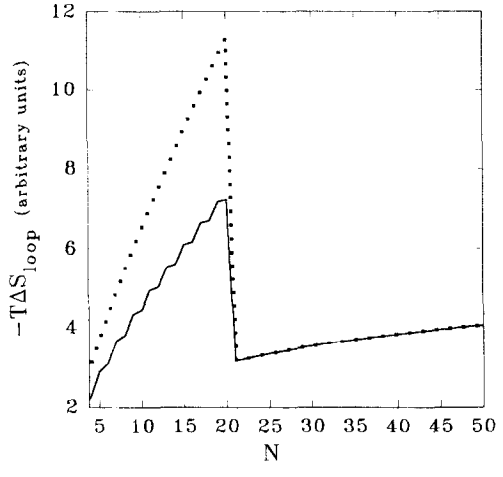

Fig. 1. Profile of the barrier to formation ($-T\Delta S_{\text{loop}}$) versus loop size in the absence (dotted line) and in the presence of magnesium (solid line). The critical loop size is assumed to be $N_0 \approx 20$.

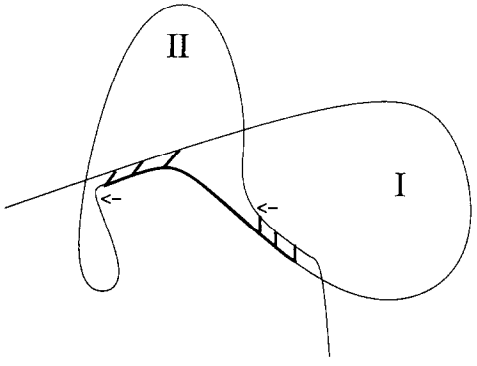

Fig. 2. Spatial representation of a pseudoknot comprising hairpin loop I followed by loop II. The formation of a pseudoknot occurs when residues in a hairpin loop engage in further base-pairing with residues outside the hairpin forming an additional stem and loop region [14]. The region to be oriented concurrently with closure of loop II is displayed in thin line between the arrows. The thick line region common to loops I and II is already oriented upon formation of loop I and prevents both loops from being coplanar.

II in between the arrows, as indicated in the figure. In this way, our simple orientational arguments reveal the necessity for the pseudoknot to acquire a truly three-dimensional (non-coplanar) structure and allows us to evaluate the kinetic barrier associated to the formation of such a motif.

However, in the case that the size of at least one of the two loops comprising the pseudoknot were beyond the critical range, there would be no orientational restriction to the coplanarity of both loops since the phosphates in the common region would always be able to find a solvent domain with bulk-like features.

2.2. *Role of magnesium ions*

It is known that Mg(II) binds in a "weak" form to adjacent phosphates of unpaired nucleotides by forming a chelate complex [15]. This fact can be casted within the orientational approach by considering each pair of adjacent coordinated phosphates of the RNA molecule as a single entity. Therefore, the effect of Mg(II) is reflected in the value of $-T\Delta S_{\text{orient}}$ for the process of phosphate orientation concurrent with loop closure which is roughly reduced by one half since the 30 kcal mol^{-1} released when a single coordination bond is formed can be actually invested in the orientation of the phosphate adjacent to the one already coordinated. This reasoning is corroborated further by the minimal (0.1 kcal mol^{-1}) difference between the free energy of formation of a bulge loop of size one and size two [16] (the size one loop does not require magnesium while in the size two loop, chelating coordination makes both phosphates behave as a single entity). In summary, we adopt the working hypothesis that the kinetic barrier strictly associated to phosphate pair orientation is reduced by one half.

In this way, loops of size equal or below the critical size will see their barriers to formation reduced by the presence of Mg(II) ions since their closure involves the orientation of their phosphate groups. However, although the presence of Mg(II) ions may affect the collision cross-section in excluded volume effects, the barrier of formation of loops beyond the critical size will not be altered by the presence of magnesium. This is so since formation of such loops do not entail the orientation of phosphate groups upon which Mg(II) can act.

The effect of Mg(II) ions on the kinetic barriers associated to the formation of simple loops can ve viewed by contrasting the shape of the profile of $-T\Delta S_{\text{loop}}$ versus N in the absence and in the presence of magnesium (Fig. 1). For loops of size greater than the critical size, there is no significant change since there is no orientational entropy loss in the formation of these loops and $-T\Delta S_{\text{loop}} \approx \mu RT \ln N$. But for loops of size equal or smaller than the critical, the kinetic barriers are reduced in the presence of magnesium and can be calculated as $-T\Delta S_{\text{loop}} \approx \mu RT \ln N + (N/2)RT \ln 2$ in the case of loops of even size and $-T\Delta S_{\text{loop}} \approx \mu RT \ln N + ((N+1)/2)RT \ln 2$ in the case of loops of odd size. This is so since for loops of even size, chelating coordination of unpaired adjacent phosphate groups reduces the number of polar entities to be oriented by one half, while for loops of odd size, there are $(N-1)/2$ coordinated entities and one extra unpaired phosphate to be oriented.

Given the exponential dependence of the mean time of loop formation on barrier size, the presence of Mg(II) ions drastically affects the formation of contacts which involve the closure of loops of length equal or below the critical size. Indeed, some of

these contacts would not be able to form within biologically relevant timescales in the absence of magnesium. These considerations reveal why some RNAs cannot properly fold to their active conformation in the absence of magnesium. This is precisely the case of the group I introns we study in the following section.

With the extentions developed in the last part of this section, the theory is now apt to be implemented in an algorithm to determine kinetic folding pathways for group I introns which can be contrasted with experimental evidence. This will be done in Section 3. Now, for the sake of completeness, we describe the kinetic Monte Carlo simulations we performed.

2.3. Monte Carlo simulations

The folding of the RNA chain follows an stochastic process (ξ) which is determined by the activation energy barriers required to form and dismantle stabilizing interactions. Thus, at each instant, the partially folded chain undergoes a series of disjoint elementary events with transition probabilities dictated by the unimolecular rates of the events. Since the choice of the set of disjoint events at each stage of folding is independent of the history that led to that particular stage of the process, the stochastic process is Markovian. The process is mechanistically constructed as follows: for each time $t \in I$, we define a map $t \to J(x,t) = \{j: 1 \le j \le n(x,t)\}$, where $J(x,t)$ is the collection of elementary events representing conformational changes which are feasible at time t given that the initial conformation has been chosen at time $t = 0$, and $n(x,t)$ is the number of possible elementary events at time t. Associated to each event there is a unimolecular rate constant $k_j(x,t)$, the rate constant for the jth event which may take place at time t for a process that starts with conformation x. The mean time for an elementary refolding event is the reciprocal of its unimolecular rate constant. Thus, for a fixed time interval I, the only elementary events allowed are elementary refolding events that satisfy $k_j(x,t)^{-1} \le |I|$. We now introduce a random variable $r \in [0, \sum_{j=1}^{n(x,t)} k_j(x,t)]$, uniformly distributed over the interval. Let r^* be a particular realization of r arising in a simulation of the process, then there exists an index j^* such that

$$\sum_{j=0}^{j^*-1} k_j(x,t) < r^* \le \sum_{j=0}^{j^*} k_j(x,t)$$

$$(k_0(x,t) = 0 \text{ for any } x,t) \tag{4}$$

This implies that the event $j^* = j^*(x,t)$ is chosen at time t for the folding process that starts at conformation x. Thus, the map $t \to j^*(x,t)$ for fixed initial condition x constitutes a realization of the Markov process which determines the folding pathway ξ_x. In turn, the probability that the j^* event is chosen at time t is

$$\frac{k_{j^*}(x,t)}{\sum_{j' \in J(x,t)} k_{j'}(x,t)}$$

Explicit values of the unimolecular rate constants require an updated compilation of the thermodynamic parameters at renaturation conditions. These parameters are used to generate the set of kinetic barriers associated to the formation and dismantling of stabilizing interactions, the elementary events in our context of interest. Thus, the activation energy barrier for the rate-determining step in the formation of stabilizing interactions is $-T\Delta S_{\text{loop}}$. The loops involved in these interactions may be of four admissible classes: bulge, hairpin, internal or pseudoknotted. For a fixed number N of unpaired bases in the loop, we shall assume the kinetic barrier to be the same for any of the four possible types of loops. This assumption is warranted since the two overlapping effects responsible for the loss in conformational entropy (the excluded volume and the orientational effects) are independent of the type of loop. Furthermore, this assumption is in relatively good agreement with calorimetric measurements. However, the activation energy barrier associated with dismantling a stem is $-\Delta H(\text{stem})$, the amount of heat released due to base-pairing and stacking when forming all contacts in the stem.

For completeness we shall display the analytic expressions for the unimolecular rate constants. If the jth step or event happens to be a helix decay process, we obtain:

$$k_j = f n \exp[G_h/RT] \tag{5}$$

where f is the kinetic constant for base pair formation after a nucleating event leading to helix formation (estimated at 10^6 s^{-1}), n is the number of base pairs in the helix formed in the jth step and G_h is the (negative) free energy contribution resulting from stacking of the base pairs in the helix. Thus, the essentially entalpic term $-G_h = -\Delta H$ (stem) should be regarded as the activation energy for helix disruption. However, if the formation of an admissible stabilizing interaction happens to be the event designated by the jth step, the inverse of the mean time for the transition will be given by:

$$k_j = fn \exp\left[-\Delta G_{loop}/RT\right] \quad (6)$$

where $\Delta G_{loop} \approx -T\Delta S_{loop}$ is the change in free energy due to the closure of the loop concurrent with helix formation.

3. Results and discussion

With the incorporation of the considerations made in Section 2 we apply the SMEL-based algorithm in order to elucidate the folding pathways followed by the group I introns *sunYL*-13 and *tdL*-7 [12]. The results concerning the times of formation of the different conserved helices are given in Table 1. Fig. 3 shows the secondary structures of both ribozymes generated in 100 s $\approx 10^6$ Monte Carlo steps by the SMEL-based algorithm. The structures obtained are identical to the philogenetically inferred ones [12]. We display the results for both the *sunYL*-13 and the *tdL*-7 ribozymes and only discuss in detail the case of the *sunYL*-13 since both cases are analogous. It becomes apparent from direct examination of Table 1 that the role of Mg(II) is paramount to reduce the kinetic barriers making them compatible with the biologically relevant timescales (approximately 1 min) and that the P7-P3 pseudoknot is formed sequentially and cooperatively. The involvement of Mg(II) during completion of pseudoknot formation (the occurrence of P3) essentially leads to a reduction of the rate-determining step to the orientation of eleven phosphate-chelated complexes, as indicated in Table 1. The sequence of events obtained for the *sunYL*-13 ribozyme is described as follows (compare Fig. 3): in the first stage P9, P7.2 and P6a form since

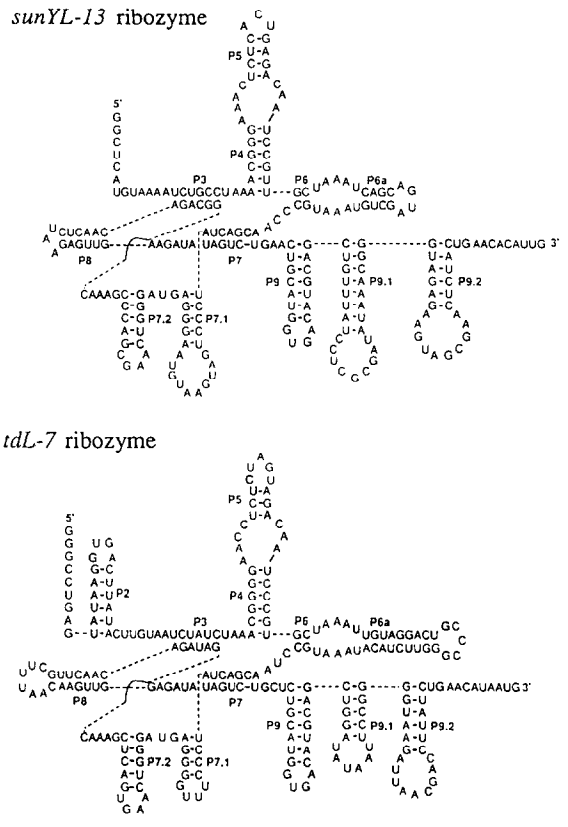

Fig. 3. Secondary structure for the *sunYL*-13 and the *tdL*-7 group I ribozymes as obtained from the SMEL-based sequential algorithm. The algorithm is rooted in a kinetically controlled Monte Carlo simulation. The simulation reproduces a Markov process in which the probability of choosing a folding event is proportional to the unimolecular rate constant associated to that event. In turn, the rate constant is proportional to Q^{-1} (see Eq. (1)).

Table 1
SMEL pathways for the *sunYL*-13 and the *tdL*-7 group I ribozymes indicating the time of formation of the different domains. The first column indicates the number of Monte Carlo steps performed by the kinetically controlled simulation

Monte Carlo steps	*sunYL*-13	*tdL*-7	Real time
10^3	P9, P7.2	P9	16.0 μs
		P2, P7.2, P7.1	20.0 μs
	P6.a	P6.a, P5	0.1 ms
10^4	P8, P5, P4	P8, P9.1	8.0 ms
	P9.1	P4	10.0 ms
10^5	P7.1, P9.2	P9.2	22.0 ms
10^6	P7	P7	24.0 s
	P3	P3	24.0 s

they involve the closure of the smallest unstrained loops for which the inner and outer domains are differentiated (tetraloops). For these loops, magnesium coordination reduces the entropic cost to the orientation of two entities, thus reducing the kinetic barrier by one half. In the next stage the strained triloops P8 and P5 and the domains P4 and P9.1 are formed. The formation of the last ones involve the closure of loops of size seven and nine respectively which, in the absence of magnesium would imply a great entropic cost. Magnesium complexation of adjacent phosphates reduces the number of entities to be oriented to four and five respectively bringing the mean time of formation of these domains to approximately 10 ms. The domains P7.1 and P9.2 involve the closure of loops of size ten. Magnesium-aided folding of these domains occurs within 22 ms. The occurrence of P8, P7.1 and P7.2 shorten the size of the loop to be closed in order to form P7 (the first stem of the pseudoknot). In that way, the loop to be closed falls well within the critical range ($N = 20$). In spite of these unfavourable conditions, this stem is formed in 24 s because of the assistance of Mg(II) ions which lower the total orientational barrier to that of a size-eleven loop. It is important to note that in the absence of Mg(II) ions, P7 could not be formed within relevant timescales of the order of minutes. In turn, the occurrence of P7 induces the formation of P3. The number of phosphates to be oriented to form P3 is reduced by fifteen. This is so because eight phosphate groups common to both P3 and the previously formed P7 have already been oriented as well as the seven phosphates forming part of the P7 helix (see Fig. 3). Thus, P3 formation entails orientation of six groups overall divided in two single stranded regions both of length three. Mg(II) participation simplifies the orientational task reducing the conformational entropy loss to that comprising overall orientation of four phosphate-chelated entities. Here we have considered that the P6 domain had already been formed. But the contact that realizes this domain is a weak contact, comprising only two base-pairs. So, there might exist an equilibrium between two conformations: one with P6 formed and the other with P6 open. In this last case, the size of the loop to be closed in order to complete the pseudoknot (P3) falls beyond the critical size and there is no orientational restriction to the coplanarity of the two loops comprising the pseudoknot. The equilibrium between the two conformations might be regulated by magnesium since further "strong" binding of magnesium to a specific site of the non-coplanar conformation might drive the equilibrium towards this conformation. In any case, the pseudoknot formation is readily completed in 24 s, well within experimental timescales for such ribozymes [3]. Our results reveal that the formation of the rate-limiting step in the P3-P7 pseudoknot formation, occurs sequentially, cooperatively and with magnesium participation in the reduction of the orientational entropy cost.

Although a body of experimental evidence concerning the kinetics of folding of large RNAs is still lacking, recent experimental work [3] is in accord with the picture expounded. The kinetics of Mg(II)-induced folding of the group I tetrahymena L-21 sca I ribozyme was probed by hybridization of complementary oligodeoxynucleotides. The formation of the P3-P7 pseudoknot was found to be the overall rate-limiting step occurring approximately within the minute timescale but, although P3 and P7 were formed approximately within the same time scale, it was not possible to decide whether the two domains formed cooperatively, sequentially or independently. This issue has now been elucidated by our work, and the specific role of Mg(II) in lowering the entropic cost associated to pseudoknot formation has been quantified and rationalized. In accord with our results, further binding of magnesium at a specific "strong" site in order to lock the pseudoknot in space was found to be fast in comparison with Mg(II)-aided folding and therefore, activity was found to switch on at almost the same time at which the domains P3 and P7 became inaccessible to the probes [3].

Acknowledgements

A.F. is principal investigator of CONICET, the National Research Council of Argentina. This work was performed during the tenure of a J.S. Guggenheim Memorial Foundation Fellowship awarded to A.F. Financial support from Fundación Antorchas (Argentina) is gratefully acknowledged.

References

[1] T.E. Creighton, Understanding protein folding pathways and mechanisms, in L.M. Gierasch and J. King (Eds.), Protein Folding, American Association for the Advancement of Science, Washington D.C., 1990, pp. 157–170.
[2] O.B. Ptytsin and G.V. Semisotnov, The mechanism of protein folding, in B.T. Nall and K.A. Dill (Eds.), Conformations and Forces in Protein Folding, American Association for the Advancement of Science, Washington D.C., 1991, pp. 155–168.
[3] P.P. Zarrinkar and J.R. Williamson, Science, 265 (1994) 918.
[4] C. Levinthal, J. Chim. Phys. (Paris), 65 (1968) 44.
[5] A. Fernández, J. Stat. Phys., 77 (1994) 1079.
[6] A. Fernández, J. Math. Chem., 17 (1995) 401.
[7] A. Fernández, Phys. Rev. Lett., 64 (1990) 2328 .
[8] A. Fernández, Phys. Rev. A: Rapid Comm., 45 (1992) R8348.
[9] A. Fernández, Physica A, 201 (1993) 557.
[10] A. Fernández, G. Appignanesi and H. Cendra, Chem. Phys. Lett., 242 (1995) 460.
[11] A. Fernández, Eur. J. Biochem., 182 (1989) 161.
[12] F. Michel and E. Westhof, J. Mol. Biol., 216 (1990) 585.
[13] C. Cantor and P. Schimmel, Biophysical Chemistry, Vol. III, W.H. Freeman and Co., San Francisco, 1980.
[14] C.W. Pleij, K. Rietveld and L. Bosch, Nucleic Acids Res. 13, (1985) 1717.
[15] T. Pan, D. Long and O.C. Uhlenbeck, in R.F. Gesteland and J.F. Atkins (Eds.), The RNA World, Cold Spring Harbor Lab. Press, Cold Spring Harbor, NY, 1993, Chapter 12, pp. 221–302.
[16] J.A., Jaeger, D.H. Turner and M. Zucker, Proc. Natl. Acad. Sci. USA, 86 (1989) 7706.